

A Compact Triple-Notch Band Ultra-Wideband Antenna

Munirah Az Zahra Abdul Rashid¹, Shaharil Mohd Shah^{2,*}, Asmarashid Ponniran¹

¹Faculty of Electrical and Electronic Engineering, Universiti Tun Hussein Onn Malaysia, Malaysia

²Research Centre for Applied Electromagnetics, Universiti Tun Hussein Onn Malaysia, Malaysia

Received July 25, 2019; Revised October 3, 2019; Accepted December 10, 2019

Copyright©2019 by authors, all rights reserved. Authors agree that this article remains permanently open access under the terms of the Creative Commons Attribution License 4.0 International License

Abstract This paper proposed a compact ultra-wideband (UWB) antenna ($17.5 \times 20.5 \text{ mm}^2$) with a triple-notch band characteristic to overcome the interference caused by the three narrow frequency bands that coexist within the ultra-wideband frequency ranging from 3.1 to 10.6 GHz as stipulated by the Federal Communication Commission (FCC). Two slots on the radiating patch and a copper trace on the ground plane of the antenna were introduced to reject the WiMAX, WLAN and SHF frequency bands. The dimensions of the slots and copper trace are optimized to achieve the desired band rejections. The compact size of the antenna is in line with the miniaturization requirement of modern wireless communication devices but at the same time is able to support multiple wireless communication services. The simulation result shows that the antenna can function over the UWB frequency range but with band rejections on the WiMAX band (from 3.2 GHz to 3.6 GHz, WLAN band) (from 5.15 GHz to 5.85 GHz) and SHF band (from 7.25 GHz to 8.395 GHz). The proposed antennas are simulated and designed in CST Microwave Studio[®] software and fabricated on a FR-4 substrate with a relative dielectric constant, ϵ_r of 4.5, loss tangent, $\tan \delta$ of 0.019 and thickness, h of 1.6 mm.

Keywords Ultra-Wideband (UWB), Triple-Notch Band, Worldwide Interoperability for Microwave Access (WiMAX), Wireless Local Area Network (WLAN), Super High Frequency (SHF)

1. Introduction

In 2002, Federal Communication Commission (FCC) in the United States has licensed the ultra-wideband (UWB) frequency spectrum to operate between the frequency range of 3.1 GHz to 10.6 GHz with Effective Isotropic

Radiated Power (EIRP) to be less than -41.4 dBm/MHz [1-2]. UWB system is widely used in applications such as medical sensing, military and indoor multipath wireless propagations [3-6]. In addition, UWB antenna has become an emerging technology that promises high speed data rate, extremely low spectral power density, slight cost and low complexity for short range communication [7-13]. However, there are other narrowband for other communication applications within the UWB frequency spectrum which are Wireless Interoperability for Microwave Access (WiMAX) between 3.2 GHz to 3.6 GHz, Wireless Local Area Network (WLAN) between 5.15 GHz to 5.85 GHz and SHF bands between 7.27 GHz to 8.395 GHz [14-17]. These three bands will cause interference to the neighboring channels that will affect the UWB communication system performance [18-20].

A traditional way of using radio frequency filters has been implemented to suppress these frequency bands, but they consumed more space when being integrated into other microwave circuits [21], which does not fulfill the miniaturization requirement. Various UWB antennas with a notch function have been developed for UWB communication systems, such as cutting diverse structure of the slot-shapes on the ground plane, on the radiating patch or etching Split Rings Resonator (SRR) in the feed line [22-27]. These methods are found useful and efficient in generating UWB frequency range and are still applied until now. However, the challenge is now focusing on miniaturising the size of the antenna but at the same time, still able to support multiple frequency requirements of the present wireless communication technology.

In this work, a triple-notch band UWB antenna is proposed to alleviate any potential interference from the co-existence of narrowbands within the UWB frequency range [28]. Two slots and a copper trace are introduced into the radiating patch and ground plane of the antenna to reject the WiMAX, WLAN and SHF frequency bands. In addition, the compact size of the antenna ($17.5 \times 20.5 \text{ mm}^2$)

will make it the best candidate to be applied in the modern wireless communication devices that require antenna's miniaturization.

2. Research Methodology

This section explains the method used in order to obtain the results of the work, starting from the design stage until the measurement stage.

2.1. Antenna Design and Configuration

The design and simulation of the antennas in this work are performed by using CST MWS[®] software. The dimensions of the antennas are optimized to achieve the best result. At the initial stage, an UWB antenna is designed based on the microstrip patch antenna and acts as the fundamental antenna in the next stage where slots and copper trace are introduced to remove each narrowband. The first and second slots are introduced on the radiating patch of the UWB antenna to reject the WiMAX and WLAN frequency bands. A copper trace is introduced on the ground plane to remove the SHF frequency band. At the final stage, both slots and the copper trace are combined into a single UWB antenna to reject all the three narrowband applications.

2.1.1. Design of Fundamental UWB Antenna

The antenna has been optimized to operate within the UWB frequency range of 3.1 GHz to 10.6 GHz. The proposed UWB antenna can be seen in Figure 1 and the dimensions of the antenna are listed in Table 1. From the figure, the antenna consists of a rectangular radiating patch with a microstrip feed line. The ladder steps are introduced at the lower region of the patch closer to the feed line to increase the impedance bandwidth [29]. The radiating patch is a copper plane with a thickness of 0.035 mm. The substrate of the antenna is a FR-4 material with a dielectric constant, ϵ_r , of 4.5, loss tangent, $\tan \delta$ of 0.019 and thickness, h of 1.6 mm. The ground plane is also made up of copper plane with a thickness of 0.035 mm. Two slots are embedded on the ground plane so that the impedance bandwidth of the UWB antenna can be further increased.

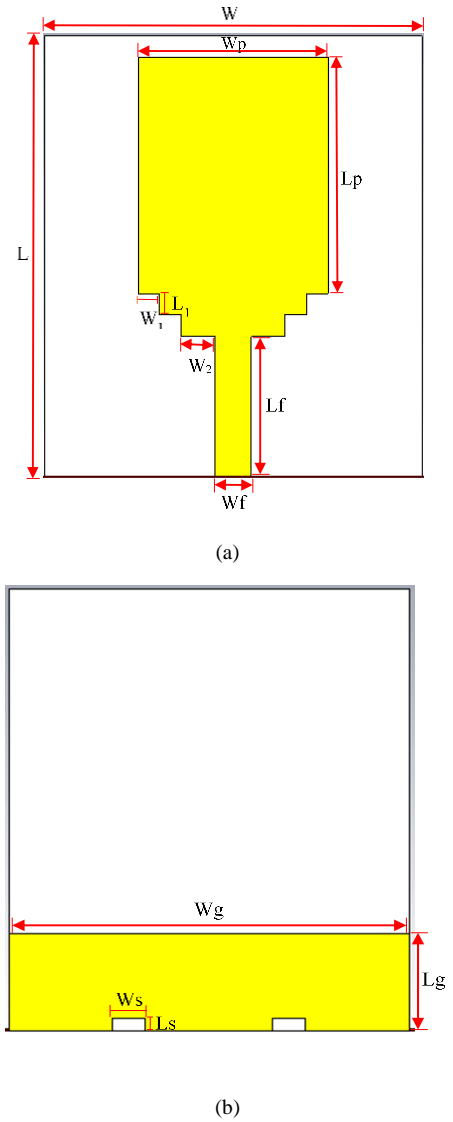


Figure 1. The proposed design of the UWB antenna

Table 1. Dimensions of the fundamental UWB antenna

Parameters	Values (mm)	Parameters	Values (mm)
L	20.5	W_s	1.4
W	17.5	W_1	1
L_p	11	W_2	1.55
W_p	8.8	L_g	4.5
L_f	6.5	W_g	17.5
W_f	1.7	L_s	0.6
L_1	1	W_s	1.4

2.1.2. Design of Fundamental UWB Antenna with a Slot to Reject the WiMAX, WLAN and SHF Frequency Bands

In this section, three antennas are designed with slots and a copper trace is introduced into each antenna to achieve three notch bands centered at 3.5 GHz (WiMAX band), 5.5 GHz (WLAN band) and 7.5 GHz (SHF band). A parametric study is performed to obtain the best location of each slot and the copper trace to achieve the desired notch band by optimising their length and width. In the final design of antenna, both slots and the copper trace are combined to reject all the narrowband applications. Figure 2 until Figure 4 show the proposed antennas with a slot on each antenna to reject the WiMAX and WLAN frequency bands, and a copper trace on the ground plane to reject the SHF frequency band. Figure 5 shows the final design of antenna which combined both slots and the copper trace. Table 2 lists the dimensions of all antennas proposed in this work.

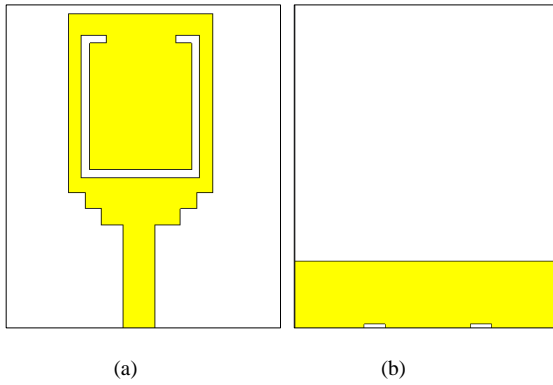


Figure 2. The UWB antenna with the first slot to reject WiMAX band; (a) Top view (b) Bottom view

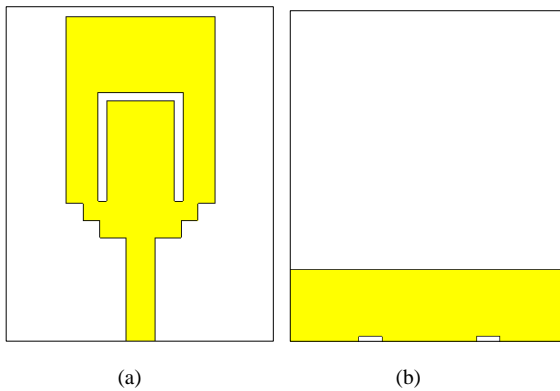


Figure 3. The UWB antenna with the second slot to reject the WLAN band; (a) Top view (b) Bottom view

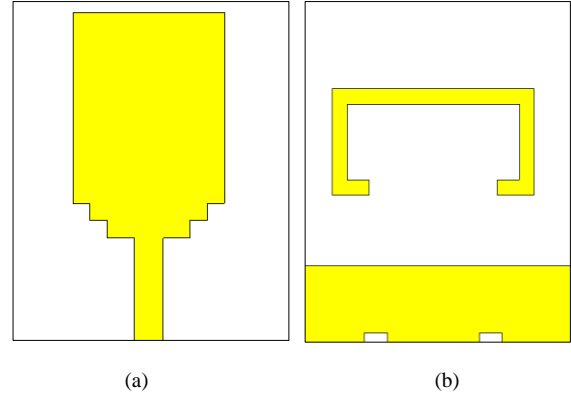


Figure 4. The UWB antenna with a copper trace on the ground plane to reject the SHF band; (a) Top view (b) Bottom view

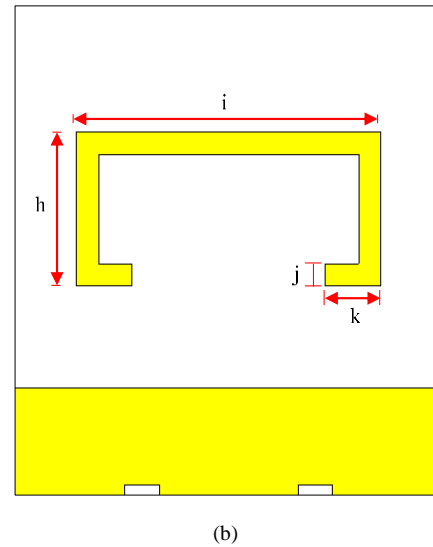
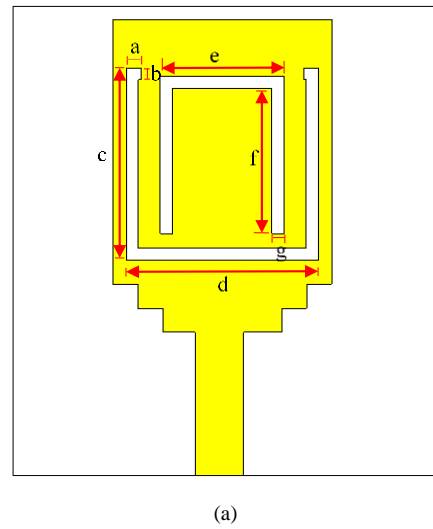


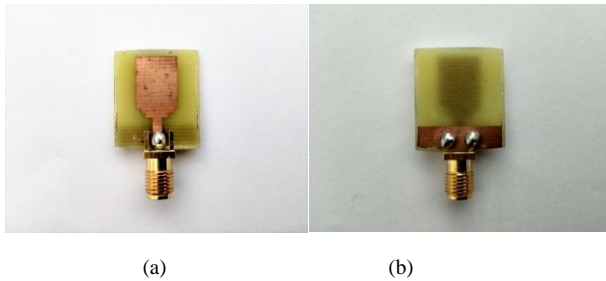
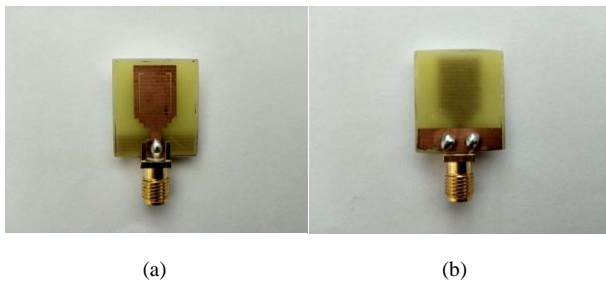
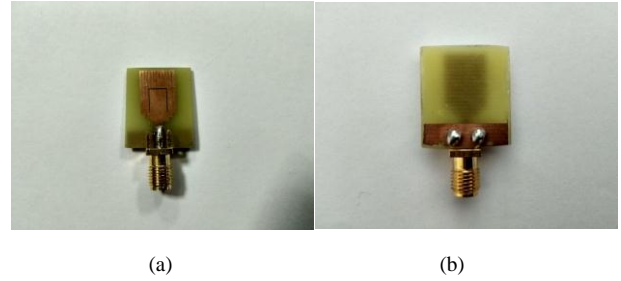
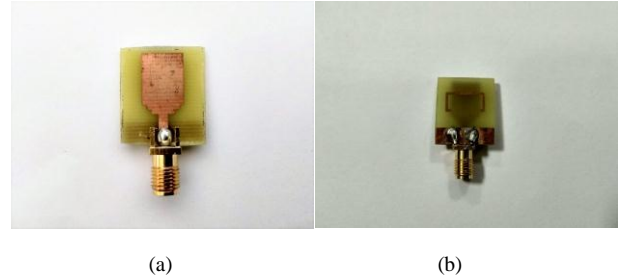
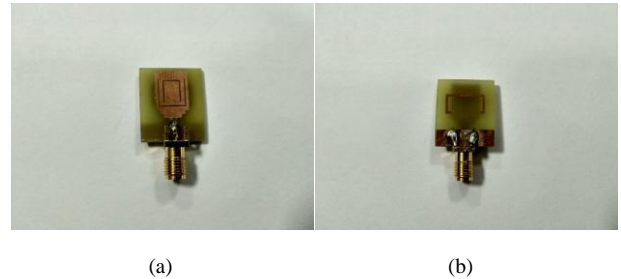
Figure 5. The UWB antenna with the combination of all the three slots; (a) Top view (b) Bottom view

Table 2. Dimensions of the UWB antenna and combination of both slots and copper trace

Parameters	Values (mm)	Parameters	Values (mm)
a	0.105	g	0.105
b	0.5	h	0.5
c	7.5	i	7.5
d	7.75	j	7.75
e	5	k	5
f	6.35	-	-

2.2. Antenna Fabrication and Measurement

The fabrication process is performed at the Advanced Printed Circuit Board (PCB) Design Laboratory. The antennas are fabricated on a FR-4 substrate with a relative dielectric constant, ϵ_r of 4.5, thickness, h of 1.6 mm and loss tangent, $\tan \delta$ of 0.019. The outcomes of the fabrication process produce five antenna prototypes as can be seen in Figure 6 to Figure 10. The antennas are then measured by using the ZVB14 Rohde & Schwarz Vector Network Analyzer (VNA). Due to the lack of facilities, only the reflection coefficients are measured in this work up to date.

**Figure 6.** Prototype of the fundamental UWB antenna; (a) Top view (b) Bottom view**Figure 7.** Prototype of the UWB antenna with the first slot; (a) Top view (b) Bottom view**Figure 8.** Prototype of the UWB antenna with the second slot; (a) Top view (b) Bottom view**Figure 9.** Prototype of the UWB antenna with the copper trace; (a) Top view (b) Bottom view**Figure 10.** Prototype of the UWB antenna with both slots and copper trace combined; (a) Top view (b) Bottom view

3. Results and Analysis

In this section, the linear characteristics of the antenna and its surface current distribution are discussed and analysed.

3.1. The Fundamental UWB Antenna

The simulation result of reflection coefficient and bandwidth of the fundamental UWB antenna and the comparison with the measurement result are shown in Figure 11. From the figure, it can be seen from the simulation result that the proposed antenna operates within 2.96 GHz to 11.11 GHz with a bandwidth of 8.15 GHz. The measurement result, on the other hand, shows that bandwidth decreases to 4.4 GHz with the frequency range from 4.80 GHz to 9.20 GHz. The discrepancy can be attributed to the fabrication tolerance and cable losses.

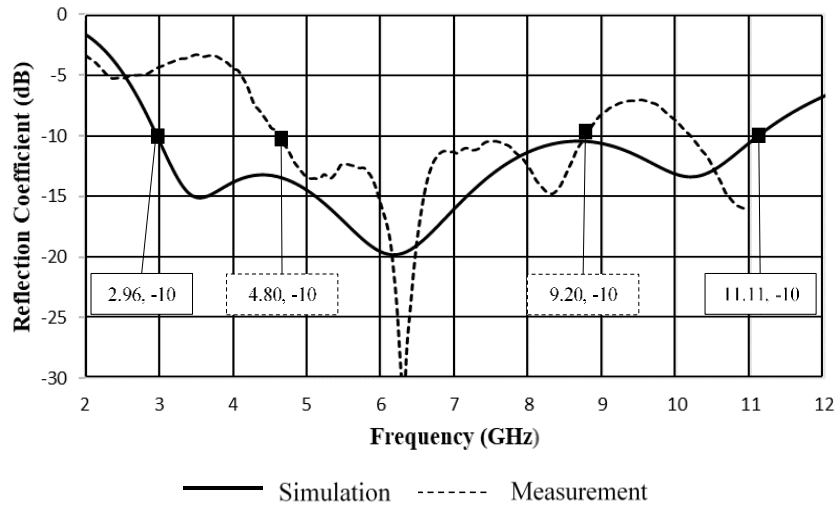


Figure 11. Comparison between the simulated and measured reflection coefficients of the UWB antenna

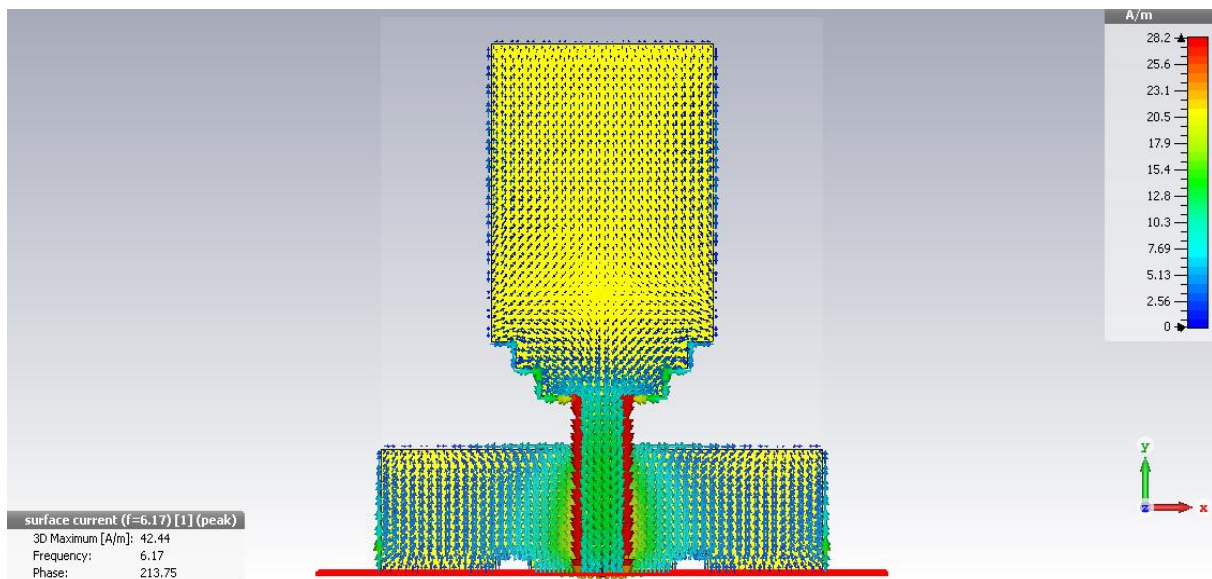


Figure 12. Surface current distribution of the simulated UWB antenna at 6.17 GHz

Figure 12 shows the surface current distribution of the UWB antenna is at 6.17 GHz. The frequency of 6.17 GHz is chosen as it is the location of the greatest reflection coefficient within the simulated frequency range. From the figure, maximum surface current is seen to be concentrated around the edges of the antenna feed line.

3.2. UWB Antenna with the First Slot (WiMAX Notch Band)

The comparison between the simulated and measured reflection coefficients of the UWB antenna with the

WiMAX notch band can be viewed in Figure 13. From the simulation result, it is observed that the antenna operates at the UWB frequency spectrum with a notch at the WiMAX band from 3.08 GHz to 4.20 GHz. The bandwidth of the notch band is 1.12 GHz. Meanwhile, the measurement result shows that the antenna has a notch band from 3.58 GHz to 4.84 GHz with the bandwidth of 1.26 GHz. Although there is an enlargement in the bandwidth of the notch band, the actual WiMAX frequency band from 3.2 GHz to 3.6 GHz is still covered.

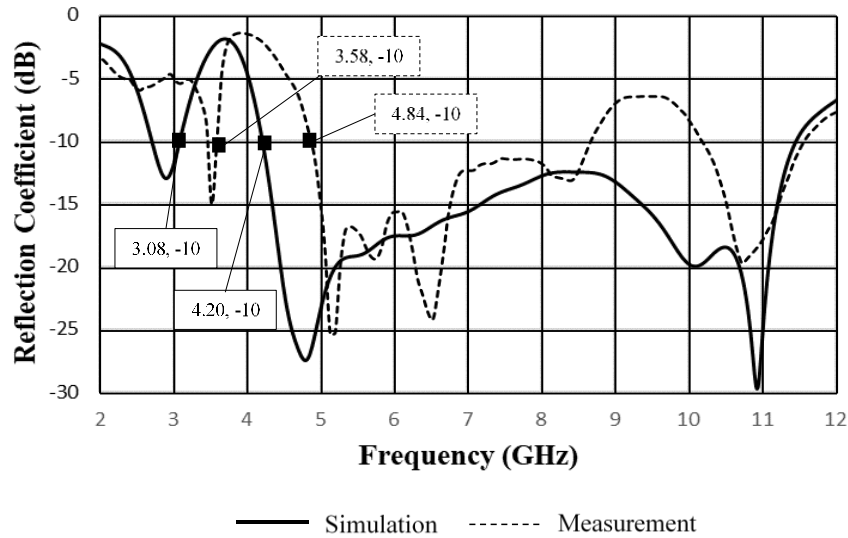


Figure 13. Comparison between the simulated and measured reflection coefficients of the UWB antenna with the first slot

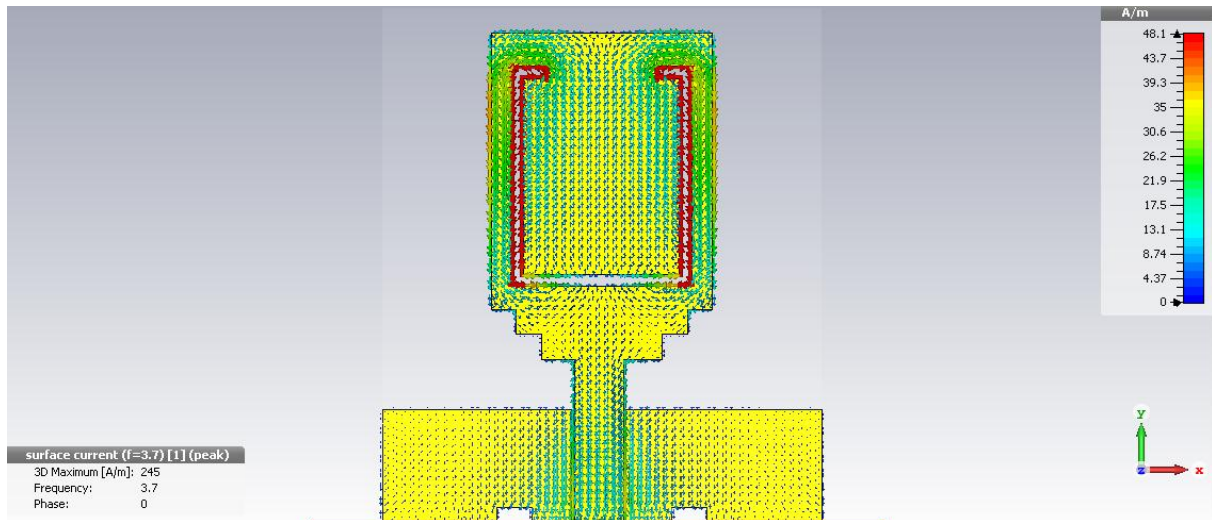


Figure 14. Surface current distribution of the simulated UWB antenna with the first slot at 3.70 GHz

Figure 14 shows the surface current distribution of the UWB antenna at 3.70 GHz. The frequency of 3.70 GHz is chosen as it is the point of lowest reflection coefficient within the notch band. From the figure, the observed maximum surface current is concentrated around the edges of the slot of the antenna. This shows that the slot is responsible for the rejection of WiMAX band.

3.3. UWB Antenna with the Second Slot (WLAN Notch Band)

The simulated and measured reflection coefficients of the UWB antenna with the second slot to reject the WLAN band can be viewed in Figure 15. From the figure, it is observed that the antenna will not operate within the frequency range of 5.13 GHz to 5.87 GHz based on the simulation result and 5.18 GHz to 5.99 GHz based on the measurement result. The actual WLAN frequency band is from 5.15 GHz to 5.85 GHz.

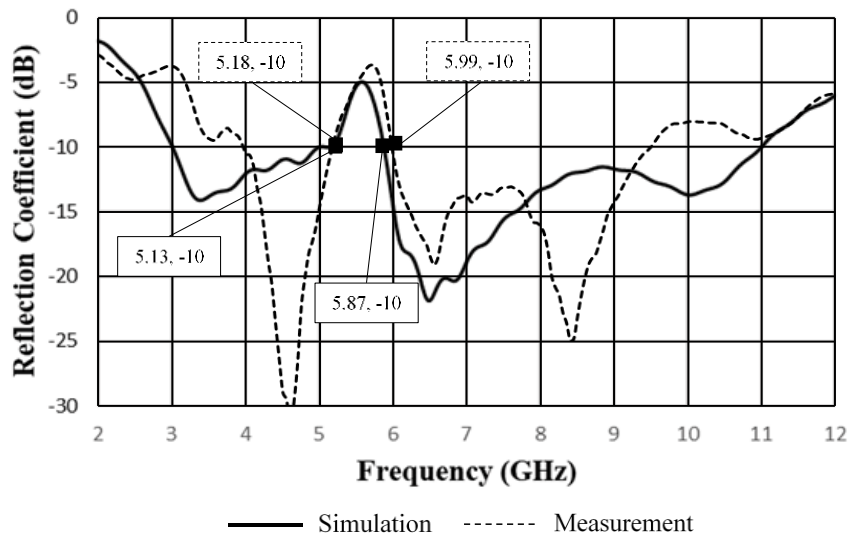


Figure 15. Comparison between the simulated and measured reflection coefficients of the UWB antenna with the second slot

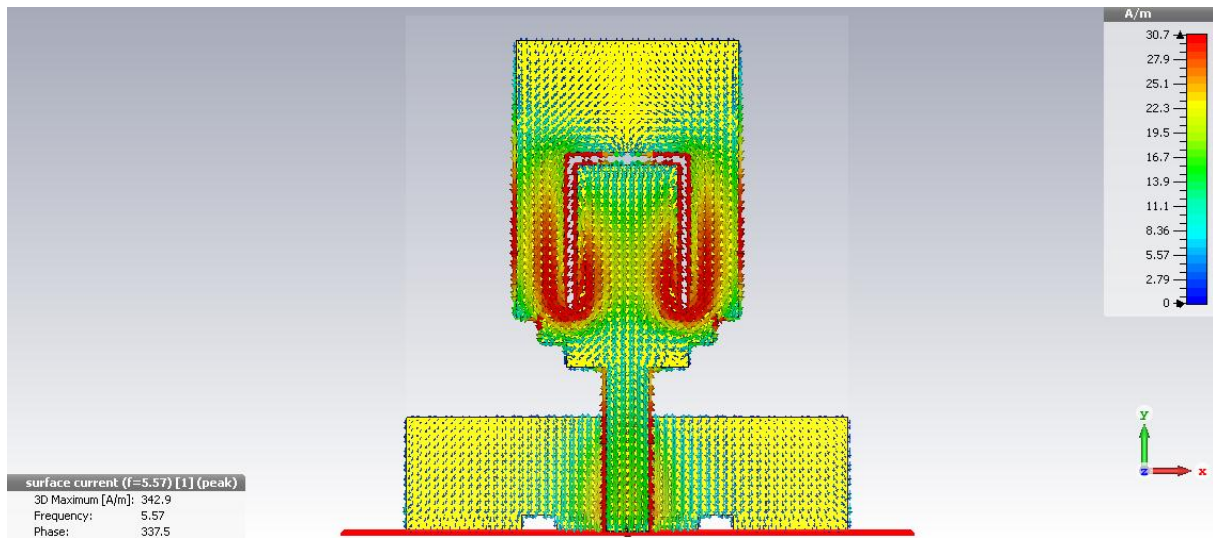


Figure 16. Surface current distribution of the simulated UWB antenna with the second slot at 5.57 GHz

Figure 16 shows the surface current distribution of the antenna at 5.57 GHz which is chosen from the fact that it is point of lowest reflection coefficient within the notch band. From the figure, the maximum surface current is seen to be concentrated around the edges of the slot of the antenna. Therefore, it is shown that the slot is accountable for the rejection of WLAN band.

3.4. UWB Antenna with the Copper Trace (SHF Notch Band)

The simulated and measured reflection coefficients of

the UWB antenna with a copper trace on the ground plane are compared and can be viewed in Figure 17. From the simulation result, it is observed that the antenna operates at the UWB frequency spectrum with a notch at the SHF band which is from 7.0 GHz to 8.9 GHz. The bandwidth of the notch band is 1.9 GHz. Meanwhile, the measured result shows that the antenna will not operate at the frequency range of 7.23 GHz until 8.39 GHz which are slightly different from the simulated result. However, the notch band from the measurement result still covers the actual SHF frequency band from 7.25 GHz to 8.395 GHz.

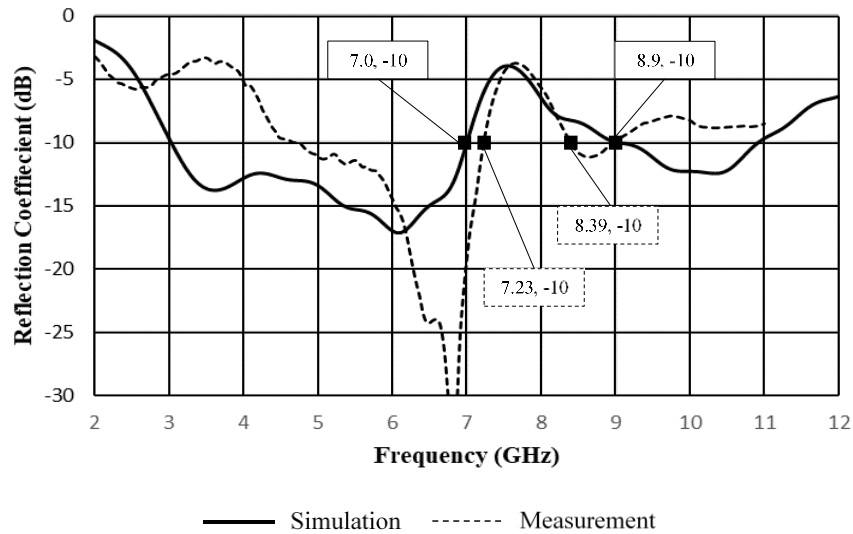


Figure 17. Comparison between the simulated and measured reflection coefficients of the UWB antenna with the copper trace

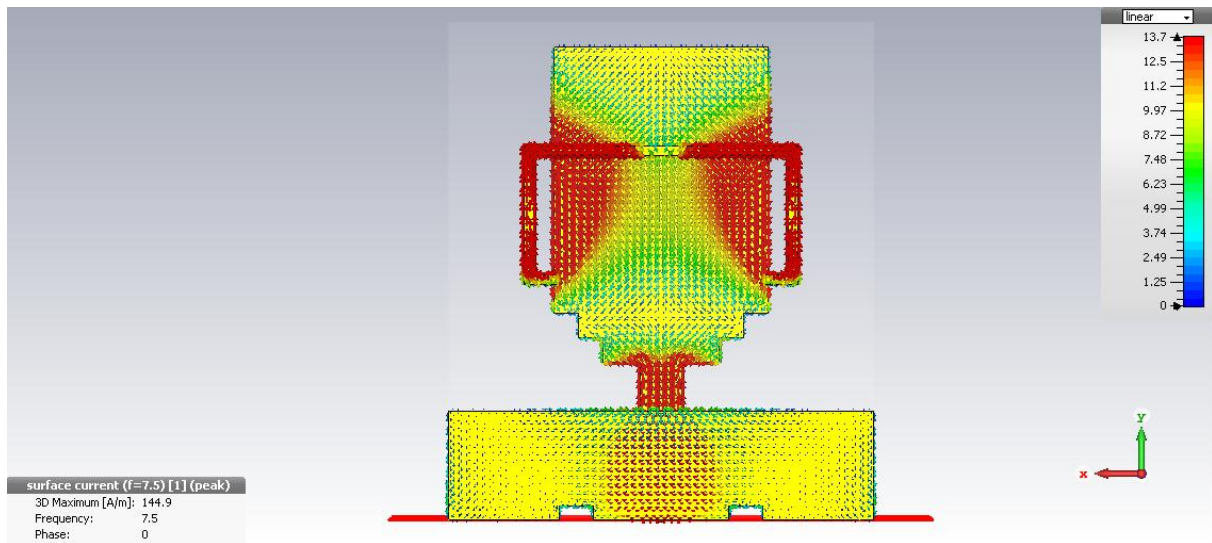


Figure 18. Surface current distribution of the simulated UWB antenna with the copper trace at 7.5 GHz

Figure 18 shows the surface current distribution of the UWB antenna at 7.5 GHz which is the point of lowest reflection coefficient. From the figure, maximum surface current is observed to be concentrated on the copper trace, around the middle edges at the side of the patch and on the feedline. Therefore, the copper trace is shown to be responsible for the SHF band rejection.

3.5. UWB Antenna with the Combination of Two Slots and Copper Trace

The simulated and measured reflection coefficients of the UWB antenna with the combination of two slots and

copper trace are compared and can be viewed in Figure 19. From the simulation result, it is observed that the antenna operates within the UWB frequency range but with a notch at the WiMAX, WLAN and SHF bands which is from 2.86 GHz to 3.64 GHz, 5.16 GHz to 5.89 GHz and from 7.24 GHz to 8.48 GHz. The bandwidth of each notch band is 0.78 GHz, 0.73 GHz and 1.24 GHz. Meanwhile, it can be observed from the measured reflection coefficient that the antenna operates within the UWB frequency spectrum with a notch from 3.58 GHz to 4.97 GHz, 5.38 GHz to 6.95 GHz and from 7.40 GHz to 8.53 GHz. The bandwidth of each notch band is 1.39 GHz, 1.57 GHz and 1.13 GHz.

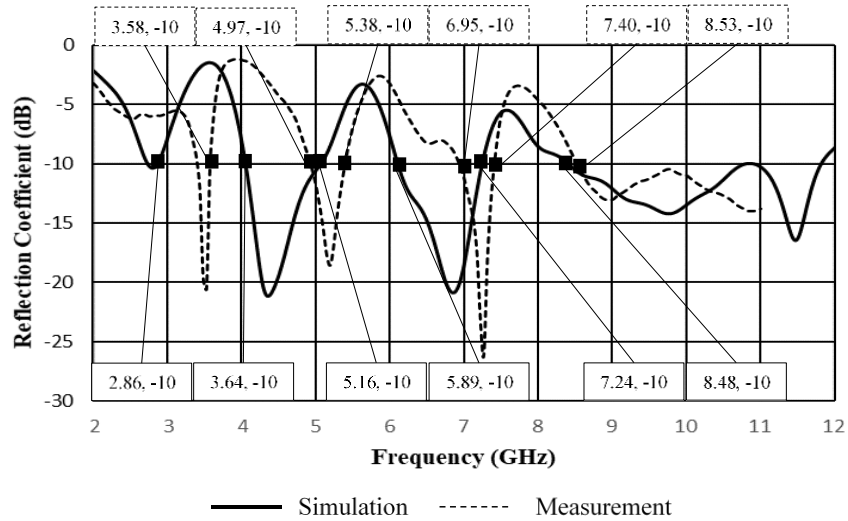
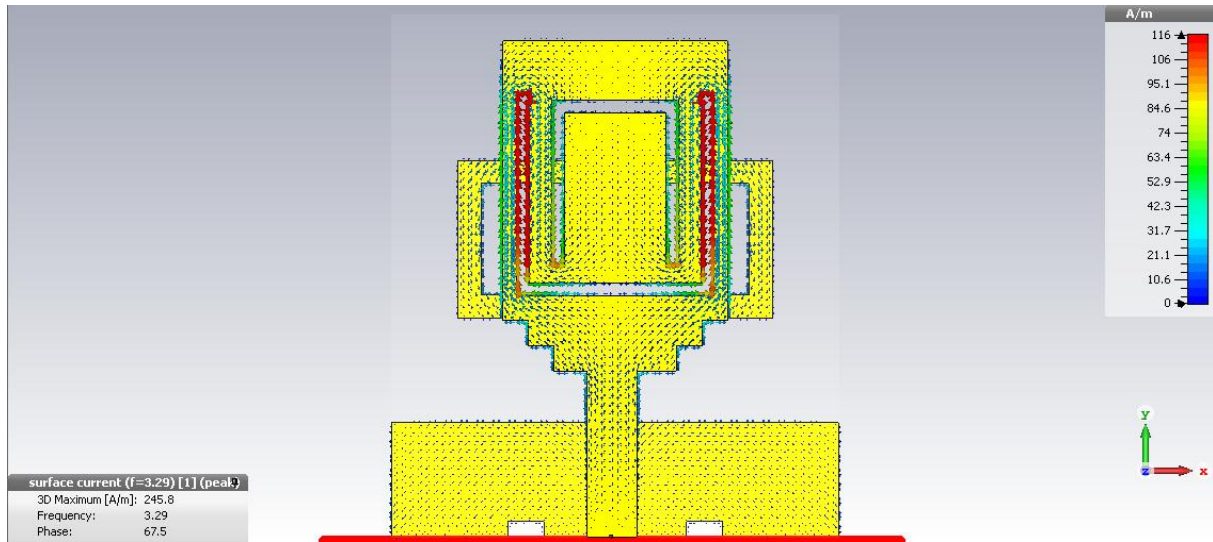
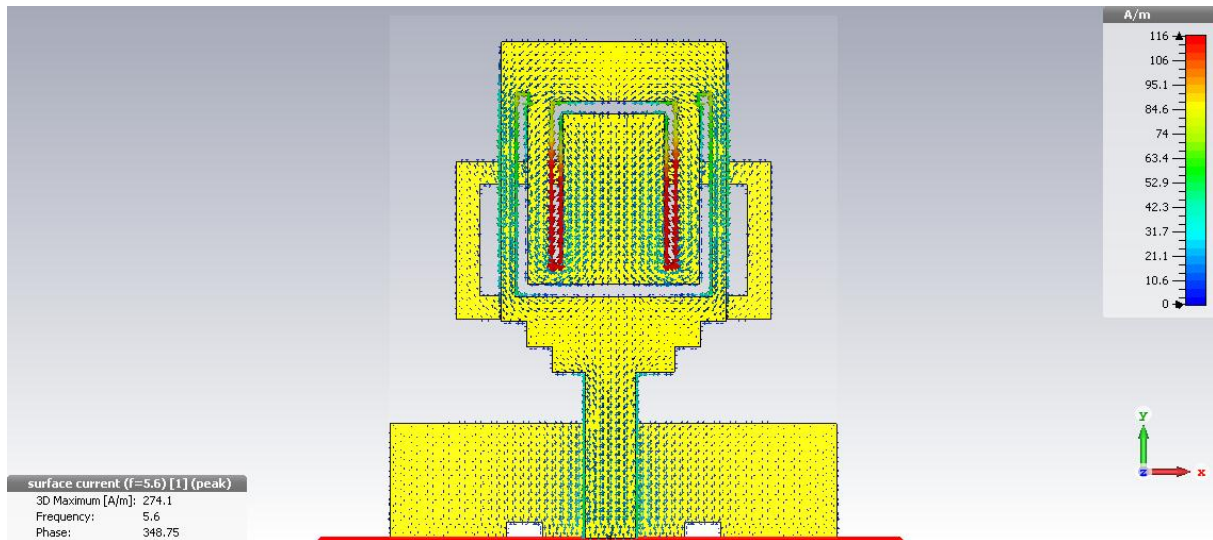


Figure 19. Comparison between the simulated and measured reflection coefficients of the UWB antenna with the combination of both slots and copper trace

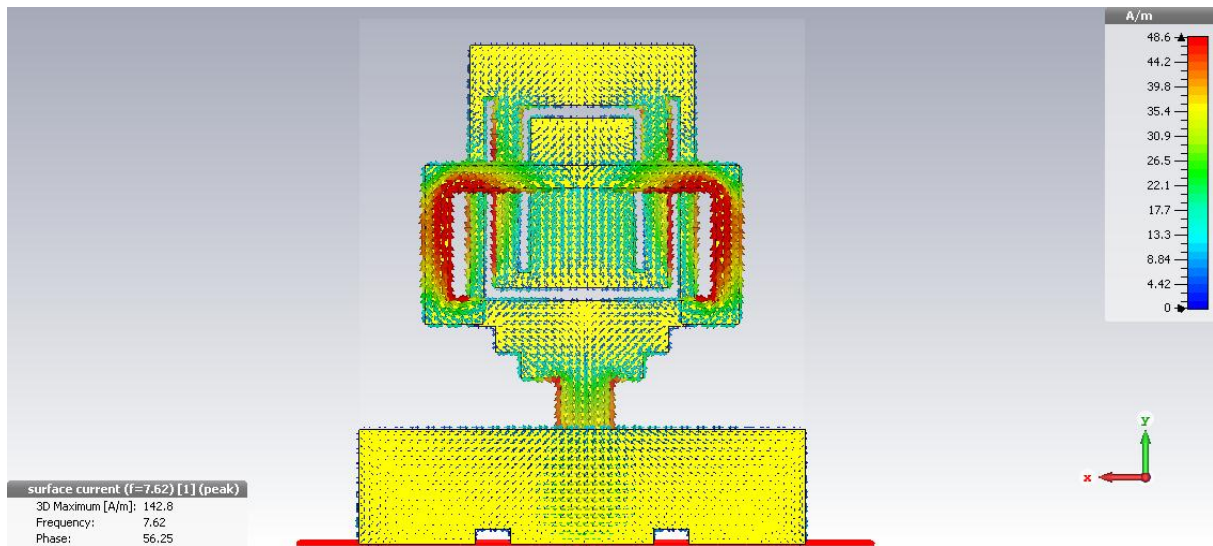
Figure 20 shows the surface current distribution of the UWB antenna at 3.29 GHz, 5.60 GHz and 7.62 GHz which are the center frequency of each notch band. From the figure, it can be observed that maximum surface current is concentrated around the edges of each slot on the radiating plane (Figure 20(a) and 20(b)) which is responsible for the WiMAX and WLAN band rejections, and also on the copper trace which is responsible to notch the SHF band (Figure 20(c)).



(a)



(b)



(c)

Figure 20. Surface current distribution of the UWB antenna with a triple-notch band centered at; (a) 3.29 GHz (b) 5.60 GHz (c) 7.62 GHz

4. Conclusions

A compact size UWB antenna ($17.5 \times 20.5 \text{ mm}^2$) with a triple-notch band is proposed in this work. Two different slots and a cop-per trace are introduced on the antenna's structure as notch filters to reject the unwanted frequency bands of WiMAX, WLAN and SHF. The simulation result demonstrates that the antenna can operate within the UWB frequency range from 2.96 GHz until 11.11 GHz and it is able to notch the WiMAX band from 3.08 GHz to 4.20 GHz (Actual WiMAX band: 3.2 GHz to 3.6 GHz), WLAN band from 5.13 GHz to 5.87 GHz (Actual WLAN band: 5.15 GHz to 5.85 GHz) and SHF band from 7.0 GHz until 8.9 GHz (actual SHF band: 7.25 GHz to 8.395 GHz). The antenna is measured on the ZVB14 Rohde & Schwarz Vector Network Analyzer.

Acknowledgements

The author would like to acknowledge Universiti Tun Hussein Onn Malaysia for the funding of this work under the Internal Grant of Tier 1 (Vote No: H247).

REFERENCES

- [1] "Federal Communication Commission First Order and Report: Revision of Part 15 of the Commission's Rules Regarding UWB Transmission Systems." pp. 98–153, 2002.
- [2] R. Patel, P. Patel, J. Lalwani, M. Sarkar, and S. Nagaraj, "Investigating the feasibility of multiple UWB transmitters in brain computer interface (BCI) applications," in 2016 IEEE 13th International Conference on Wearable and Implantable Body Sensor Networks (BSN), pp. 236–241, 2016.
- [3] Y. Zang, K. Pahlavan, Y. Zheng, and L. Wang, "UWB gesture detection for visually impaired remote control," in 10th International Symposium on Medical Information and Communication Technology (ISMICT), pp. 1–4, 2016.
- [4] R. Thai-Singama, F. Du-Burck, and M. Piette, "A UWB generator based on a ECL Monostable one-shot for ETSI communications and Military radar applications," in International Conference on Advanced Technologies for Communications (ATC 2014), pp. 663–668, 2014.
- [5] Z. Chen, Y. Liu, S. Li, and G. Wang, "Study on the multipath propagation characteristics of UWB signal for indoor lab environments," in 2016 IEEE International Conference on Ubiquitous Wireless Broadband (ICUWB), pp. 1–4, 2016.
- [6] R. A. Fayadh, F. Malek, H. A. Fadhil, and N. Saudin, "Design of ultra wideband rectangular microstrip notched patch antenna," in 2013 IEEE International Conference on Control System, Computing and Engineering, pp. 408–412, 2013.
- [7] J. Gomes, "N-dimensional Pulse Shape and Position Modulation for high speed UWB communication," in International Conference on Circuits, Systems, Communication and Information Technology Applications (CSCITA), pp. 126–131, 2014.
- [8] R. M. Edwards and S. Villarreal-Reyes, "UWB spectral line analysis and suppression in low rate UWB radio," in IET Seminar on Wideband and Ultrawideband Systems and Technologies: Evaluating current Research and Development, pp. 1–5, 2008.
- [9] A. Toccafondi, D. Zampilli, C. D. Giovampaola, and V. Tesi, "Low-power UWB transmitter for RFID transponder applications," in IEEE International Conference on RFID-Technologies and Applications (RFID-TA), pp. 234–238, 2012.
- [10] M. Garbati, R. Siragusa, E. Perret, and C. Halopé, "Low cost low sampling noise UWB Chipless RFID reader," in IEEE MTT-S International Microwave Symposium, pp. 1–4, 2015.
- [11] S. Zhang, R. Han, W. Huang, S. Wang, and Q. Hao, "Linear Bayesian Filter Based Low-Cost UWB Systems for Indoor Mobile Robot Localization," in IEEE SENSORS, 2018, pp. 1–4, 2018.
- [12] S. Sapienza, M. Crepaldi, P. M. Ros, A. Bonanno, and D. Demarchi, "On Integration and Validation of a Very Low Complexity ATC UWB System for Muscle Force Transmission," IEEE Trans. Biomed. Circuits Syst., vol. 10, no. 2, pp. 497–506, 2016.
- [13] X. Guan et al., "Novel ultra-wideband antenna with dual-band rejection characteristic for wearable applications," in IEEE International Workshop on Electromagnetics: Applications and Student Innovation Competition (iWEM), pp. 1–3, 2016.
- [14] Y. Zeng, H. Zhang, Y. Zhang, and H. Zhao, "Compact Band-Notched UWB Antenna Based on CSRR for WiMAX/WLAN Applications," in International Conference on Microwave and Millimeter Wave Technology (ICMMT), pp. 1–3, 2018.
- [15] W. Ahmad and D. Budimir, "UWB filtennas with dual bandnotch for WiMAX and WLAN bands using circular and square resonators," in Active and Passive RF Devices Seminar, pp. 1–3, 2016.
- [16] B. Hammache, A. Messai, I. Messaoudene, M. A. Meriche, M. Belazzoug, and F. Chetouah, "Reconfigurable triple notched-band ultra-wideband antenna," in 12th International Conference on Innovations in Information Technology (IIT), pp. 1–5, 2016.
- [17] D. T. Nguyen, D. H. Lee, and H. C. Park, "Very Compact Printed Triple Band-Notched UWB Antenna With Quarter-Wavelength Slots," IEEE Antennas Wirel. Propag. Lett., vol. 11, pp. 411–414, 2012.
- [18] Y. Jalil, C. Chakrabarty, and B. Kasi, "A Compact Wideband Microstrip Antenna Intergrated with Band-Notched Design," vol. 77, 2012.
- [19] A. Sudhakar, M. Satyanarayana, M. S. Prakash, and S. K. Sharma, "Frequency notched antenna to overcome EMI between UWB systems and Wireless Local Area Networks (WLANs)," in 13th International Conference on Electromagnetic Interference and Compatibility (INCEMIC), pp. 170–175, 2015.
- [20] Y. Li, Q. Liu, Y. Chen, C. Li, Z. Mo, and F. Li, "A compact

- triple wideband-notched UWB antenna,” in International Workshop on Antenna Technology (iWAT), pp. 1–4, 2018.
- [21] [21] S. Habib, G. I. Kiani, and M. F. U. Butt, “An efficient UWB FSS for electromagnetic shielding,” in International Conference on Electromagnetics in Advanced Applications (ICEAA), pp. 1543–1546, 2017.
- [22] A. A. Ibrahim, H. F. A. Hamed, M. A. El-Din, A. Abdel-alla, and E. Yahia, “A compact planer UWB antenna with band-notched characteristics,” in International Conference on Engineering and Technology (ICET), pp. 1–5, 2014.
- [23] J. Wang, J. Zhao, and J. Li, “Compact UWB bandpass filter with triple notched bands using parallel U-shaped defected microstrip structure,” *Electron. Lett.*, vol. 50, no. 2, pp. 89–91, 2014.
- [24] M. Mirzaee, S. Noghianian, and B. S. Virdee, “High selectivity UWB bandpass filter with controllable bandwidth of dual notch bands,” *Electron. Lett.*, vol. 50, no. 19, pp. 1358–1359, 2014.
- [25] X. Bihui, Z. Yanwen, Z. Yuteng, and G. Li, “Compact UWB slot antenna with wideband-notched characteristics based on rectangular SRR,” in IEEE 5th Asia-Pacific Conference on Antennas and Propagation (APCAP), pp. 29–30, 2016.
- [26] J. Y. Siddiqui, C. Saha, and Y. M. M. Antar, “Compact Dual-SRR-Loaded UWB Monopole Antenna With Dual Frequency and Wideband Notch Characteristics,” *IEEE Antennas Wirel. Propag. Lett.*, vol. 14, pp. 100–103, 2015.
- [27] D. Sarkar, K. V. Srivastava, and K. Saurav, “A Compact Microstrip-Fed Triple Band-Notched UWB Monopole Antenna,” *IEEE Antennas Wirel. Propag. Lett.*, vol. 13, pp. 396–399, 2014.
- [28] H. Liu and Z. Xu, *Design of UWB Monopole Antenna with Dual Notched Bands Using One Modified Electromagnetic-Bandgap Structure*, vol. 2013, 2013.
- [29] E. J. Ali, R. Yahya, N. Abdullah, and S. Zahirah Sapuan, *Ultra-Wideband Monostatic Antenna for behind the Wall Detection*, vol. 7, 2017.